Article citation info:
Wang G., Huang S., Liang Y., Wang Y., Sun J., Liu J. 2026. A Practical Vision Framework for Robust Classification of Selected Wood Species under Low-Quality and Device-Variable Conditions. *Drewno. Prace naukowe. Doniesienia. Komunikaty.* https://doi.org/10.53502/wood-216329

Łukasiewicz Poznań Institute of Technology

Drewno. Prace naukowe. Doniesienia. Komunikaty
Wood. Research papers. Reports. Announcements

Journal website: https://drewno-wood.pl

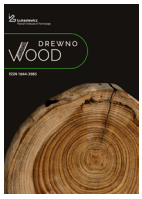

A Practical Vision Framework for Robust Classification of Selected Wood Species under Low-Quality and Device-Variable Conditions

Guona Wang[a]
Shanshan Huang[a]
Yi Liang[a]
Youming Wang[b]
Jianping Sun[a *]
Jingru Liu[c]

[a] State Key Laboratory of Featured Metal Materials and Life-cycle Safety for Composite Structures, School of Resources, Environment and Materials, Nanning 530004, China, Guangxi University
[b] School of Management and Information, Zhejiang College of Construction
[c] School of Agricultural and Animal Husbandry, Industry Development Research Institute, Guangxi University

Article info
Received: 8 July 2025
Accepted: 2 January 2026
Published: 24 June 2026

Keywords
wood recognition
computer vision
deep learning
low-quality image
image enhancement
data augmentation

The accurate identification of wood species plays a vital role in key industrial processes, such as timber processing operations, quality assurance inspections, and inventory tracking. In industrial production settings, wood specimen images are frequently acquired using cost-constrained mobile imaging devices, inevitably compromising image quality through motion-induced blurring, sensor noise artifacts, and suboptimal resolution characteristics. These technical limitations severely degrade the operational effectiveness of traditional recognition systems, creating cascading inefficiencies across downstream production workflows. To overcome these limitations, we have developed an industrial-grade deep learning framework specifically engineered to deliver reliable wood species identification under challenging real-world imaging conditions. The proposed framework incorporates two core technical components to address image quality degradation in industrial settings: (1) an enhanced Very Deep Super-Resolution (VDSR) network for detail reconstruction, and (2) a comprehensive multi-scale augmentation pipeline for robust feature learning. In this study, evaluation experiments were conducted utilizing wood image datasets of three distinct species-Pterocarpus santalinus, Pterocarpus tinctorius, and Gluta sp.-which were captured by three different imaging devices corresponding to high, medium, and low-quality acquisition conditions. The experimental validation demonstrates substantial performance gains, with our enhanced framework achieving a 25% absolute accuracy improvement over the baseline ResNet-50 model when processing low-quality input images. This research establishes a cost-effective and scalable technical foundation for quality recognition systems in industrial imaging applications, with direct integration potential into intelligent quality control systems for manufacturing operations.

DOI: 10.53502/wood-216329

* Corresponding author: jpsun@gxu.edu.cn

Introduction

Wood species identification serves as a fundamental and indispensable operation in forestry practices, with significant implications for multiple domains, including timber grading systems, quality control processes, anti-illegal logging surveillance, and biodiversity preservation initiatives (Barmpoutis et al., 2018). Traditional wood identification methods mainly consist of manual experience-based identification, anatomical feature analysis, and physicochemical-assisted identification, all of which depend heavily on expert knowledge and microscopic anatomical analysis. However, these methods are often inefficient and costly. With the advancement of computer technology, image classification has achieved significant breakthroughs in fields such as agriculture and medicine (Chen et al., 2023; Lu et al., 2024; Xu et al., 2025). For example, Grimmer et al. (2025) developed an automated riverine wood detection tool that integrates machine learning and remote sensing, enabling the quantification of parameters such as wood length and volume. In medical imaging diagnostics, advanced image processing and deep learning methods have shown remarkable efficacy in handling complex image data and enhancing recognition accuracy, providing valuable insights for the intelligent transformation of wood classification.

Early wood classification techniques were heavily reliant on manual experience and basic image processing methods. Mallik et al. (2011) achieved semi-automated wood species identification for the first time by integrating scanning electron microscopy (SEM) image segmentation with linear discriminant analysis (LDA) and support vector machines (SVM). However, their dependence on high-resolution images and manually designed statistical features constrained their generalization capabilities (Peters et al., 2025). Subsequent studies attempted to incorporate texture analysis techniques, such as gray-level co-occurrence matrices (GLCM) and local binary patterns (LBP), combined with SVM classifiers for classification (Kobayashi et al., 2019; Li et al., 2017; Souza et al., 2020). Although these methods yielded satisfactory results under specific conditions, their robustness in complex environments (e.g., lighting variations, noise interference) remained limited (Huang et al., 2024). For instance, Riana et al. (2021) demonstrated that when using K-means segmentation and GLCM feature extraction to identify defects in mahogany, classification performance significantly deteriorated if the wood surface exhibited stains or wear. Furthermore, these methods often required specialized equipment (e.g., X-ray or high-resolution microscopes), hindering their deployment on low-cost, portable devices (Peters et al., 2025).

The emergence of deep learning has initiated an era of deep feature learning for wood classification (Wang et al., 2021). Convolutional neural networks (CNN) automatically learn hierarchical image features through multi-layer nonlinear transformations, overcoming the limitations of manual feature engineering and showcasing significant advantages in wood classification (Ravindran et al., 2018; Wu et al., 2021). Subsequently, Prabu et al. (2020) further developed the open-source XyloTron system, which integrates multi-light imaging with CNN models to enable rapid on-site classification of wood and wood products, thereby advancing the practical application of deep learning in forestry. Follow-up research has extensively explored diverse computer vision paradigms to further enhance model performance. Transfer learning strategies, utilizing architectures ranging from standard backbones to advanced models like DenseNet and Xception, have been widely adopted to mitigate data scarcity and improve training efficiency (Geovanni et al., 2022; Kırbaş & Çifci, 2022; Wu et al., 2021). Concurrently, efforts to optimize CNNs have focused on data augmentation techniques (Ergun, 2021), lightweight model designs (Ergun, 2024; Zhao et al., 2021), and novel architectures incorporating dynamic convolutions or differential features to capture complex patterns (Cai et al., 2025; Z. Zheng et al., 2024; Zheng et al., 2025). Beyond standard CNNs, Vision Transformers (ViT) have recently been introduced to capture global texture dependencies and subtle variations, marking a significant shift toward attention-based modelling in forestry (Zhang et al., 2023; Zhuang et al., 2022). Research dimensions have also been expanded through multimodal fusion of spectra and images (Pan et al., 2023) and multi-view learning strategies that fuse complementary information from different anatomical sections (Rosa da Silva et al., 2022). In the microscopic domain, advanced detection algorithms like WoodYOLO have been developed for precise cellular analysis (Nieradzik et al., 2024; X. Yang et al., 2024). Furthermore, the focus on interpretability has evolved from visualizing classification rationale (C. Zheng et al., 2024) to precise instance segmentation. For example, models like YOLOv8-seg now enable the quantification of anatomical features such as vessels and rays (Liu et al., 2025). Despite recent advancements, critical challenges persist in practical forestry applications, particularly in accurately identifying wood species from low-resolution, noise-contaminated images and addressing cross-device data discrepancies—these remain pressing obstacles to overcome in current timber image recognition systems (Collins-Key et al., 2025).

Image enhancement techniques offer a promising solution to the aforementioned challenges. In non-wood-related domains, methods such as vertex detection (Koo & Cha, 2017), homomorphic filtering (Z. Yang et al., 2024), and thermal radiation optimization (Pan et al., 2025) have substantially improved image quality and recognition performance. In wood classification,

although approaches like expectation-maximization (EM) adaptive filtering (Abdul Hamid et al., 2018) and terahertz (THz) imaging (Vijayalakshmi et al., 2024) have been utilized to enhance image quality, research on improving low-resolution wood images remains limited. Moreover, while data augmentation techniques (e.g., simple geometric transformations) have been extensively applied to address data scarcity (Ergun, 2021), the synergistic effects of combining these techniques with image enhancement methods warrant further investigation.

To tackle these challenges, this study puts forward an integrated framework that merges VDSR-based super-resolution reconstruction with multi-scale data augmentation techniques, thereby bolstering classification robustness across a spectrum of image quality levels (Fig. 1). Unlike conventional models trained on standardized clean datasets, our approach enhances model generalization capabilities through dual mechanisms: (1) quality restoration of degraded wood images and (2) strategic expansion of training data diversity. We conducted comprehensive evaluations on three visually similar timber species (*Pterocarpus santalinus*, *Pterocarpus tinctorius*, and *Gluta sp.*) under three deliberately designed acquisition scenarios that replicate authentic forestry classification conditions. The experimental results demonstrate that our method achieves significant improvements in recognition accuracy, with particularly outstanding performance on low-quality images characterized by resolution degradation and acquisition noise. This research provides a practical and cost-effective solution for intelligent wood identification while offering valuable insights for developing field-deployable timber classification systems in forestry applications.

Materials and methods

1. Data preparation

The endangered species of rosewood, *Pterocarpus tinctorius*, which is easily confused with rosewood, and *Gluta sp.*, which is similar to rosewood, were selected for this experiment. The samples were obtained from Guangdong Yuzhu Wood Testing Co., Ltd., which has a CMA qualification. Due to the strict requirement for certified reference materials of these precious species, forty-five authentic wood samples were collected for each of the three wood species, with a sample area of about 60 mm in length and 70 mm in width. To address the biological variability within this constraint, we employed multi-device acquisition and comprehensive data augmentation to mathematically model surface variations, thereby ensuring that the dataset provides sufficient feature representation for deep learning.

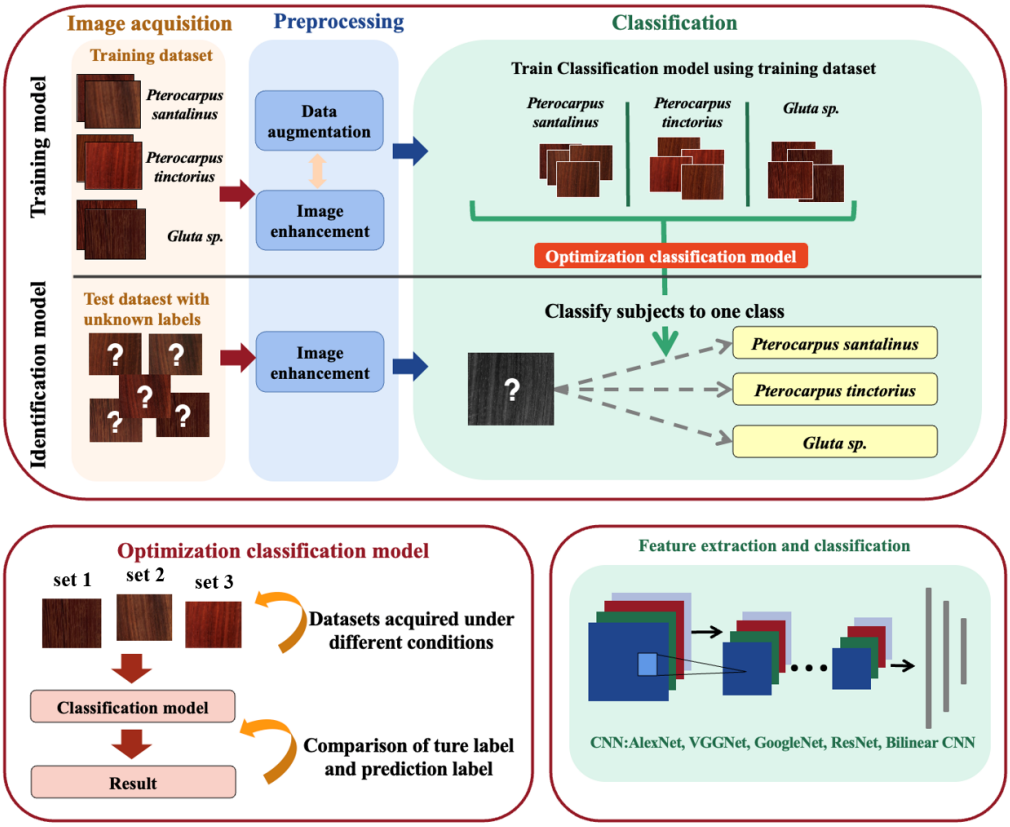

Fig. 1. The diagram of the study

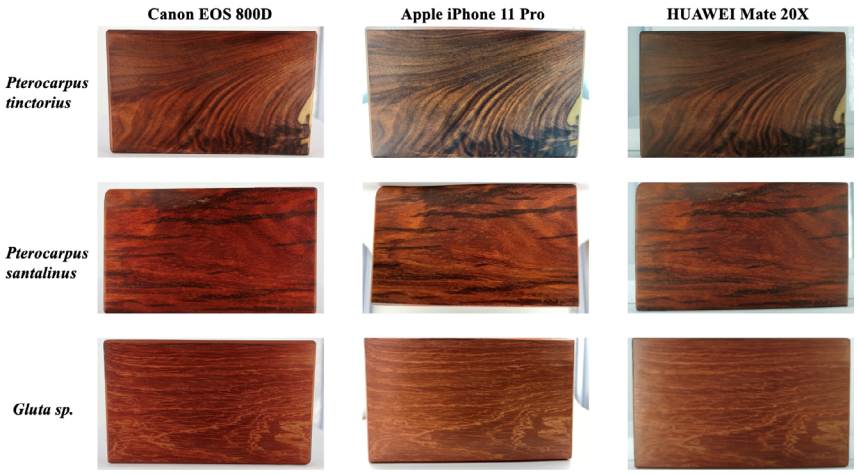

Fig. 2. Wood images in the dataset

To simulate real-world industrial conditions, this study established three datasets using distinct imaging devices. The high-quality image dataset (set 1) was captured using a CANON EOS 800D camera in a miniature studio with consistent lighting and geometry. Based on the sensor specifications covering the 70 mm-wide sample, the system achieved a spatial resolution of approximately 0.015 mm/pixel, enabling the capture of fine anatomical details. In contrast, the medium-quality (set 2) and low-quality (set 3) datasets were captured using an Apple iPhone 11 Pro and a HUAWEI Mate 20X, respectively. These images were acquired under unrestricted conditions of light, shooting distance, and angle to ensure dataset diversity and categorization difficulty (Fig. 2). Due to the handheld nature of acquisition, the spatial resolution for these sets is lower, estimated at approximately 0.032 mm/pixel and 0.036 mm/pixel, respectively.

This experimental design is intended to emulate the heterogeneous imaging environments characteristic of industrial timber operations, particularly for mobile inspection scenarios and conditions with variable image quality. It is important to note that while consumer-grade devices were utilized in this study to rigorously test the algorithm's robustness to image degradation, including noise and blur, the proposed software framework is independent of specific imaging hardware. Therefore, it can be seamlessly adapted to standard industrial cameras for continuous, high-load production line applications where durability is paramount.

2. Image enhancement

Raw images acquired from mobile devices in industrial settings often suffer from noise and blurring, which degrade discriminative anatomical features. To address this, we employed the VDSR network to reconstruct high-quality wood images. Unlike the traditional Super-Resolution CNN (SRCNN), which employs a shallow 3-layer architecture to map low-resolution images directly to high-resolution outputs, VDSR adopts a deeper 20-layer network, enabling improved learning capacity. The network utilizes cascading 3×3 convolutional kernels with a depth of D, resulting in a large receptive field calculated as (2D+1)×(2D+1). For a 20-layer network, this yields a receptive field of 41×41, allowing the model to utilize richer contextual information from the image features. To accelerate convergence in such a deep network, the learning rate was increased compared to SRCNN, and gradient clipping was employed to prevent gradient explosion.

The core mechanism of VDSR is residual learning. Instead of directly generating a high-resolution image, the network learns a residual map, which represents the high-frequency difference between the high-quality reference and the interpolated low-quality input. This approach was specifically adopted to mitigate the acquisition artifacts inherent in our mobile datasets (set 2 and set 3), such as the jagged edges along vessel pores caused by low sensor resolution and the textural blurring resulting from handheld capture. By learning these high-frequency residuals, the VDSR network recovers the structural integrity required for accurate classification.

Regarding the training strategy, the VDSR model was trained on a multi-scale dataset to handle super-resolution tasks across different magnification levels. We constructed the training set by down-sampling the high-quality images from set 1 by scale factors of 2, 3, and 4. This enables the model to robustly reconstruct wood features under varying resolution degradation scenarios.

3. Data augmentation

Given the limited number of physical wood samples, a comprehensive data augmentation pipeline was implemented to expand the dataset size and enhance

model robustness against real-world industrial variations. Unlike generic augmentation, we applied specific transformations tailored to simulate the variable conditions of wood inspection:

1. Geometric Transformations: To model the arbitrary orientation of wood logs on conveyor belts, images were subjected to random rotations of 90°, 180°, and 270°, as well as horizontal and vertical flipping. Additionally, random affine transformations were applied with a rotation range of [-15°, +15°], a scaling factor ranging from [0.8, 1.2], and a shear range of [-10°, +10°] to simulate variations in camera distance and shooting angles.
2. Image Degradation Simulation: To ensure the model could generalize to the low-quality domains (set 2 and set 3), we explicitly simulated acquisition artifacts on the high-quality training data. This included Gaussian noise injection (with a mean of 0 and a variance of 0.01) to mimic sensor noise, and Gaussian blurring (with a fixed kernel size of 3×3) to simulate motion blur and out-of-focus effects.
3. Through these operations, the diversity of the training set was significantly enriched, forcing the model to learn invariant anatomical features rather than memorizing specific sample orientations.

4. Experimental setup and model implementation

To ensure a rigorous evaluation of the mode's generalization ability and prevent data leakage, a stratified partitioning strategy was employed. Before partitioning, the low-quality images (set 2 and set 3) were pre-processed using the VDSR framework to standardize anatomical clarity across all data sources. Subsequently, each of the three datasets (set 1, set 2-enhanced, and set 3-enhanced) was individually randomly divided into three independent subsets: 70% for training, 10% for validation, and 20% for testing. Crucially, data augmentation was exclusively applied to the training subsets after partitioning. This approach generated a large-scale, diverse training corpus while ensuring that the validation and test sets contained only original, unseen images, thereby allowing for an unbiased assessment of performance across different image quality levels.

To systematically evaluate the impact of network depth and structural mechanisms on wood species recognition, this study selected seven representative CNN architectures for benchmarking. These include classical convolutional architectures (AlexNet, VGGNet 16), multi-branch networks (GoogleNet), residual networks of varying depths (ResNet 18, ResNet 50, ResNet 101), and a texture-oriented model (Bilinear CNN) known for fine-grained classification. Comparative experiments were conducted across these models to identify the most effective backbone for the proposed framework.

All experiments were conducted on a workstation equipped with an NVIDIA GPU using the PyTorch deep learning framework. During the training phase, the Stochastic Gradient Descent (SGD) optimizer was employed to minimize the Cross-Entropy Loss. The hyperparameters were uniformly configured for all models to ensure fair comparison: an initial learning rate of 0.01 (with a decay factor of 0.1 every 30 epochs), a momentum of 0.9, and a batch size of 128. The models were trained for 100 epochs, and the weights yielding the highest accuracy on the validation set were saved for final testing.

Evaluation methodology

1. Image quality evaluation

In this study, Peak Signal to Noise Ratio (PSNR) and Structural Similarity Index Measure (SSIM) are used as image quality evaluation metrics. The Mean Squared Error (MSE) and PSNR are calculated as follows:

$$MSE = \frac{1}{MN}\sum_{i=1}^{M}\sum_{j=1}^{N}[I(i,j) - K(i,j)]^2 \quad (1)$$

$$PSNR = 10\,log\frac{MAX^2}{MSE} \quad (2)$$

Where I(i,j) and K(i,j) represent the pixel values of the original high-quality reference image and the reconstructed image at position (i,j), respectively. M and N denote the height and width of the image. MAX is the maximum possible pixel value of the image. A larger PSNR value indicates better reconstruction quality.

Compared with PSNR, SSIM better reflects the structural similarity between the reference and reconstructed images. It is calculated as:

$$SSIM(x,y) = \frac{(2\mu_x\mu_y+C_1)(2\sigma_{xy}+C_2)}{(\mu_x{}^2+\mu_y{}^2+C_1)(\sigma_x{}^2+\sigma_y{}^2+C_2)} \quad (3)$$

Where and are the mean intensities of images x and y; and are their respective variances; and is the covariance. and are small constants used to avoid instability when the denominator is close to zero. The SSIM value ranges from -1 to 1, with 1 indicating perfect structural identity.

2. Model evaluation method

The performance of the classification models was evaluated using Accuracy (A), Precision (P), Recall (R), and F1-score based on the confusion matrix. The calculation formulas are as follows:

$$A = \frac{\sum_{i=1}^{n} N_{ii}}{\sum_{i=1}^{n} \sum_{j=1}^{n} N_{ij}} \quad (4)$$

$$P_i = \frac{N_{ii}}{\sum_{k=1}^{n} N_{ki}} \quad (5)$$

$$R_i = \frac{N_{ii}}{\sum_{k=1}^{n} N_{ik}} \quad (6)$$

$$F1 - score_i = \frac{2 \times P_i \times R_i}{P_i + R_i} \quad (7)$$

Where n represents the number of classes (here, n=3). denotes the number of samples correctly classified into class i (True Positives). represents the number of samples belonging to class i but incorrectly classified as class j. It is important to clarify that in this study, a "sample" refers to an individual digital image (or image patch) input into the neural network, rather than a physical wood block. Thus, represents the total number of image samples predicted as class i, and represents the total number of actual image samples in class i.

Results and discussion

1. Evaluation of image enhancement effects

In this study, the performance of the VDSR method in wood image enhancement was comprehensively evaluated through systematic quantitative analysis and visual comparison.

In terms of quantitative assessment, Table 1 systematically tests the reconstruction capability of VDSR under different down-sampling scales. The results show that VDSR achieves a PSNR of 33.643 dB and a SSIM of 0.990 under the ×2 scale factor, both of which are significantly better than the Bicubic interpolation (32.704 dB, 0.987). This demonstrates that VDSR provides superior reconstruction of wood images in terms of image brightness, contrast, and structure. This advantage diminishes as the scale factor increases, and the PSNR difference narrows to 0.083 dB at ×4, indicating that VDSR is more effective in enhancing images with mild degradation.

In terms of visual quality assessment, Fig. 3 visualizes the ability of VDSR to recover wood grain features. The first row is the overall image, and the second and third rows are the local zoomed-in images. Set 2 and set 3 are overall blurred, the wood grain details are missing, and the edges of the conduits show obvious jaggedness; after the VDSR treatment (set 2-VDSR, set 3-VDSR), the image quality is significantly improved, which is mainly manifested in the following aspects: firstly, in the macroscopic scale, the reconstructed wood grain continuity is significantly improved. The original broken growth wheel structure was restored to its natural transition characteristics after VDSR; second, in the micro details, VDSR effectively restored the anatomical characteristics of the wood. The originally ambiguous conduit cross-section showed a clear cell wall structure after treatment, and the pore size and distribution pattern were accurately reconstructed. This detailed restoration is crucial for subsequent wood identification, especially for species with discriminatory conduit arrangement patterns.

It is worth noting that although the samples in Fig. 3 do not correspond exactly to the test conditions in Table 1, the two present a highly consistent trend of quality change: for better quality samples (e.g., set 2 and ×2 tests), VDSR achieves a significant visual improvement, while for the severely degraded samples (e.g., set 3 and ×4 tests), the enhancement effect is relatively limited. This consistency validates the reliability of VDSR performance.

Combining the quantitative and qualitative results reveals that VDSR outperforms traditional methods in both maintaining the structural similarity of wood grain and detail recovery, and is particularly suitable for processing mildly to moderately degraded wood images. This conclusion provides an important preprocessing basis for subsequent classification experiments.

Table 1. Image quality evaluation results: average PSNR and SSIM for scale factors (×2, ×3, ×4)

Scale	Method	PSNR (dB)	SSIM
×2	Bicubic	32.704	0.987
	VDSR	33.643	0.990
×3	Bicubic	27.597	0.962
	VDSR	27.822	0.965
×4	Bicubic	25.943	0.951
	VDSR	26.026	0.952

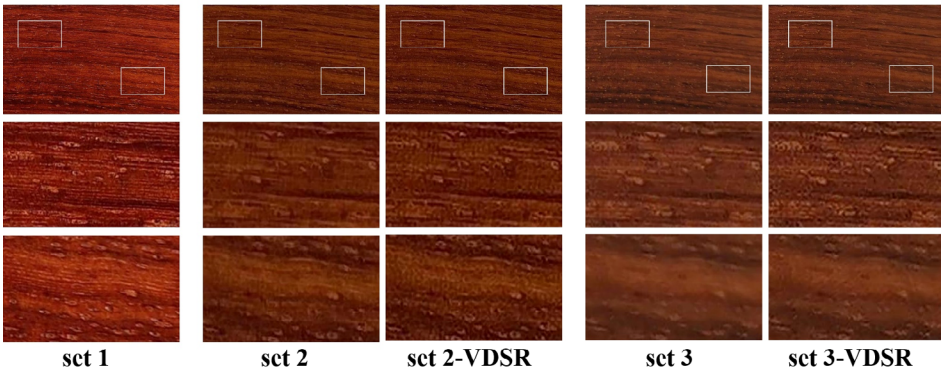

Fig. 3. Effect diagram of image reconstruction by super resolution

Impact of image quality on classification performance

1. Classification results and analysis

Comprehensive comparative experiments were conducted using the seven selected CNN models to evaluate wood species recognition performance. As shown in Fig. 4 and Table 2, ResNet 50 exhibited the best overall performance, achieving the fastest convergence speed and the highest accuracy among the evaluated architectures. Consequently, ResNet 50 was selected as the backbone for the proposed framework due to its superior capability in handling the complex features of degraded wood images.

2. Effect of image quality on classification results

In this study, we systematically analyzed the mechanism of image quality on wood recognition performance and found that the sensitivity of different tree species to image quality was significantly different. As shown in Fig. 5 and Table 3, when the evaluation shifted from the test subset of the high-quality dataset (Test set 1) to the test subset of the low-quality dataset (Test set 3), the overall accuracy of the model decreased significantly from 97.2% to 56.5%, indicating that the image quality is a key factor affecting the classification performance.

It is worth noting that there were significant differences in the sensitivity of different tree species to image quality. Among them, the F1 value of *Pterocarpus santalinus*

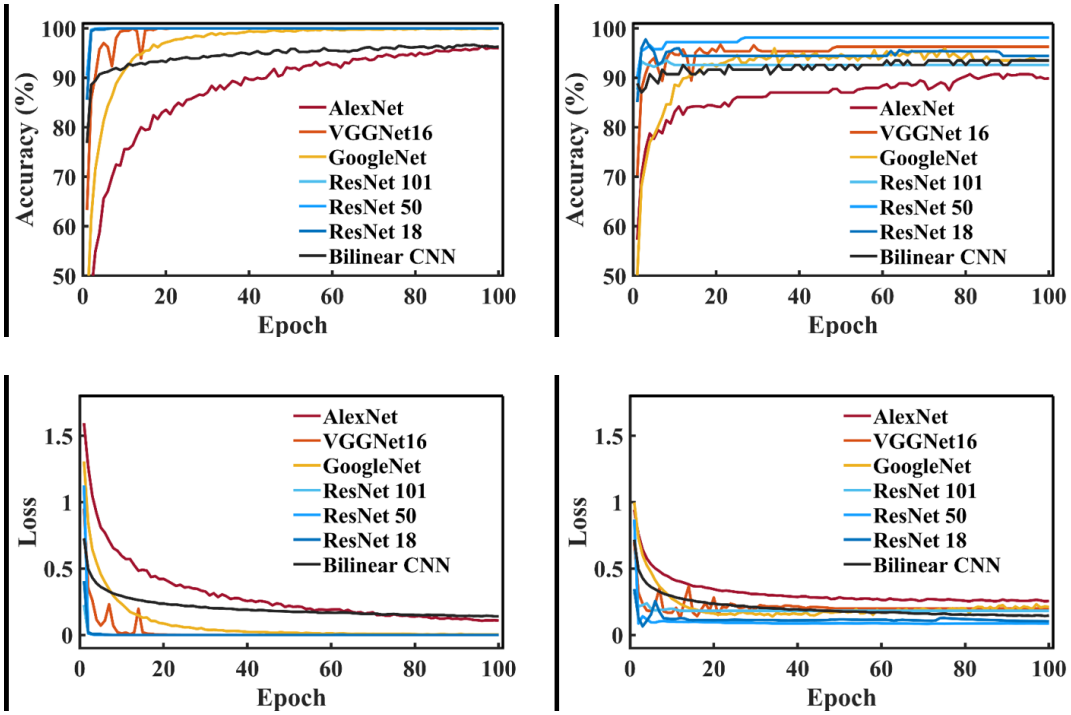

Fig. 4. The accuracy and loss curves for different deep learning models: a) represents the change in training set accuracy, b) represents the change in testing set (Test set 1) accuracy, c) represents the change in training set loss function, and d) represents the change in testing set (Test set 1) loss function

Table 2. Precision of Different Deep Learning Models (Bold for Best Model Precision)

Accuracy (%)	Training set	Test set 1	Test set 2	Test set 3
AlexNet	96.0	90.7	85.2	72.2
VGGNet 16	100.0	96.3	96.3	82.4
GoogleNet	99.9	93.5	92.6	74.1
ResNet 18	100.0	97.2	96.3	74.1
ResNet 50	**100.0**	**98.2**	**97.2**	**81.5**
ResNet 101	100.0	92.6	92.6	72.2
Bilinear CNN	96.3	93.5	88.9	88.9

Table 3. Performance Metrics of ResNet 50 Trained on Different Image Datasets

	Test set 1	Test set 2	Test set 3
Accuracy of training set (%)	100.0	100.0	100.0
Accuracy of test set (%)	97.2	73.2	56.5
P- *Pterocarpus santalinus*	0.946	0.938	0.375
R- *Pterocarpus santalinus*	0.972	0.417	0.083
F1- *Pterocarpus santalinus*	0.959	0.577	0.136
P- *Pterocarpus tinctorius*	0.971	0.875	0.692
R- *Pterocarpus tinctorius*	0.944	0.778	0.659
F1- *Pterocarpus tinctorius*	0.958	0.824	0.675
P- *Gluta sp.*	1.000	0.600	0.508
R- *Gluta sp.*	1.000	1.000	1.000
F1- *Gluta sp.*	1.000	0.750	0.674

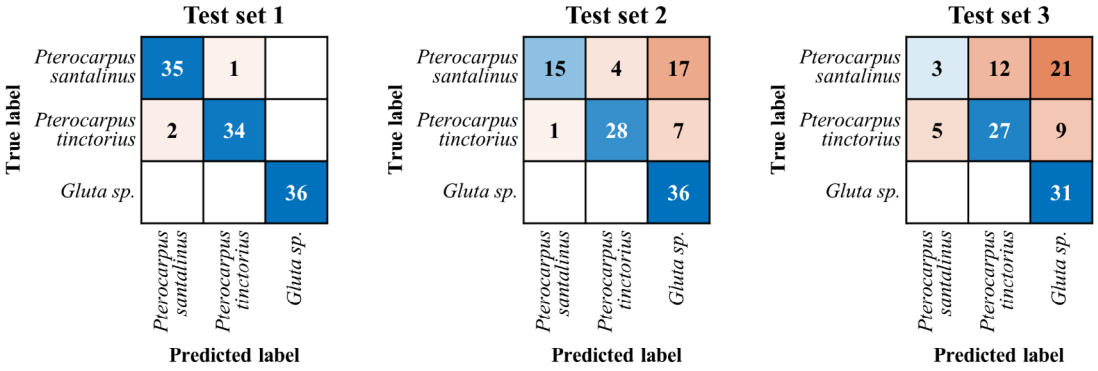

Fig. 5. Confusion matrices for different datasets

plummeted from 0.959 to 0.136, showing extremely high sensitivity; in contrast, the F1 value of *Pterocarpus tinctorius* dropped from 0.958 to 0.675, showing strong quality robustness; and the F1 value of *Gluta sp.* showed a decrease in F1 value from 1.000 to 0.674, maintaining a relatively stable identification performance.

The Grad-CAM visualization analysis (Fig. 6) revealed that this discrepancy mainly stems from the different characteristics of the discriminative features of each tree species. The recognition of *Pterocarpus santalinus* mainly relies on the specific spatial interaction pattern formed by the conduits and rays, and

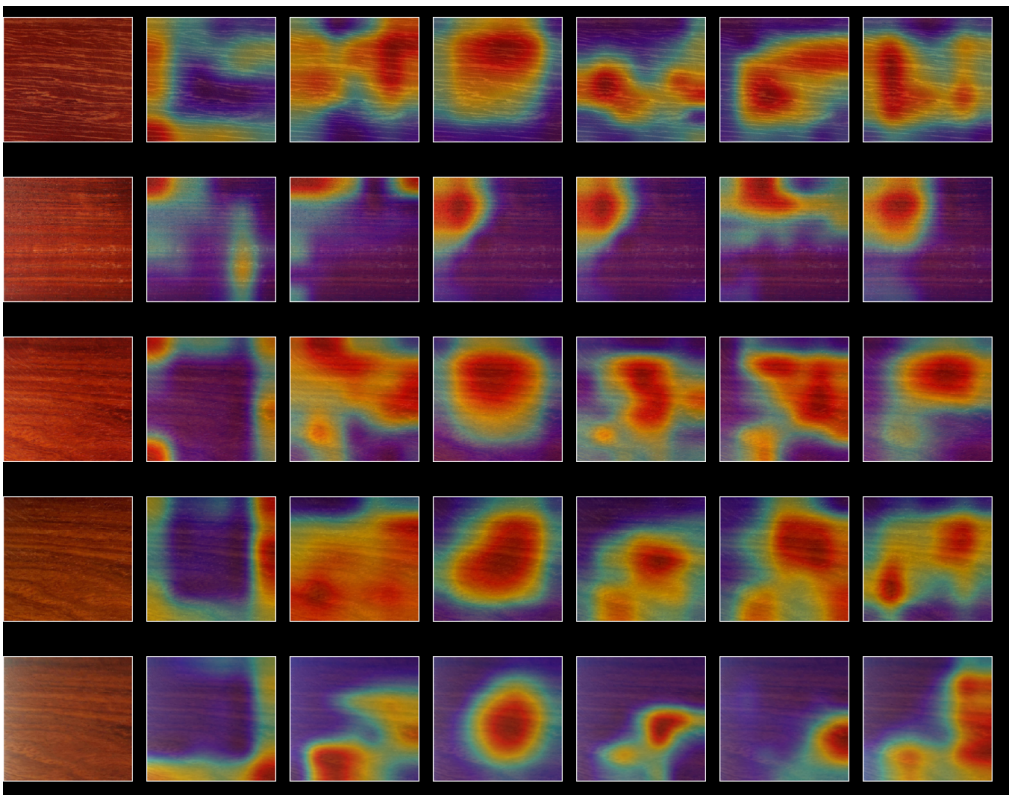

Fig. 6. Visualization of Grad-CAM: a) Visualization example of the Gluta sp. image from Test set 1, b) Visualization example of the Pterocarpus tinctorius image from Test set 1, c) Visualization example of the Pterocarpus santalinus image from Test set 1, d) Visualization example of the Pterocarpus santalinus image from Test set 2, e) Visualization example of the Pterocarpus santalinus image from Test set 3

this kind of mesoscopic scale organization-structural relationship is highly susceptible to being lost when the image is degraded. Fig. 6e clearly shows that in low-quality set 3, the model only captures localized edge features and fails to recognize complete catheter-ray spatial arrangement patterns, which directly leads to its recall plummeting from 0.972 to 0.083. In contrast, the catheter-distribution radial gradient feature relied on by *Pterocarpus tinctorius* is more stable as a statistical feature, while the *Gluta sp.*'s periodic ray cell arrangement produces high-contrast features that are partially retained when quality decreases, which allows both to maintain relatively good recognition performance in low-quality images.

The experimental results show that differentiated quality control standards need to be established for the discriminative feature characteristics of different tree species in the development of wood recognition systems. Especially for tree species relying on complex spatial features, more stringent image acquisition and processing procedures should be adopted to ensure the integrity of key discriminative features. These findings provide an important basis for the optimal design of the wood intelligent identification system.

3. Effectiveness of data preprocessing

To validate the efficacy of the proposed preprocessing pipeline (comprising VDSR image enhancement and data augmentation) in recognizing low-quality wood images, comparative experiments were conducted using the ResNet 50 backbone. As shown in Fig. 7 and Table 4, the integration of image enhancement and data augmentation yielded significant performance gains, particularly for the low-quality datasets. Specifically, while the recognition accuracy for Test set 1 (High Quality) showed only a marginal improvement from 97.2% to 98.2%—indicating that the baseline model is already robust for high-quality inputs—the improvements were substantial for the lower-quality datasets. Notably, the accuracy for Test set 2 (Medium Quality) increased markedly from 73.2% to 97.2%, and for Test set 3 (Low Quality), it surged from 56.5% to 81.5%.

These results demonstrate that the proposed preprocessing strategy effectively mitigates the impact of image degradation. VDSR successfully recovers lost texture details (e.g., vessel boundaries), while data augmentation enriches the diversity of the training distribution, thereby significantly enhancing the model's generalization ability on device-variable inputs.

Table 4. Model recognition accuracy for different image preprocessing

Accuracy (%)	Training set	Test set 1	Test set 2	Test set 3
Original data	100.0	97.2	73.2	56.5
Image enhanced	100.0	97.2	76.9	62.0
Dataset expanded	100.0	98.2	97.2	73.2
Enhanced and expanded	100.0	98.2	97.2	81.5

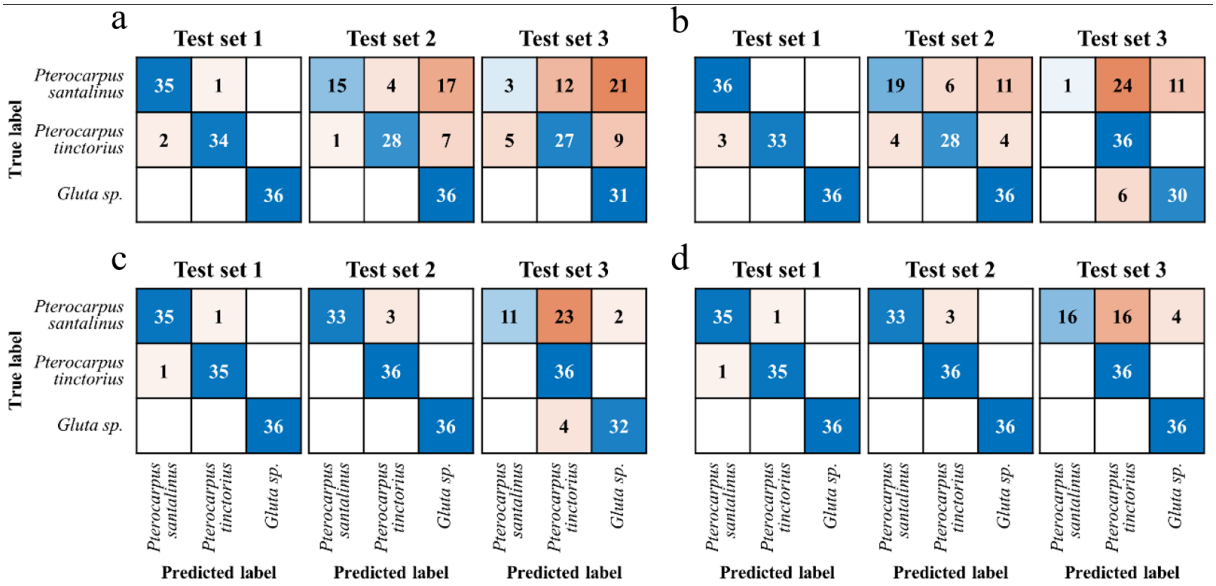

Fig. 7. Confusion matrix of different test sets after image processing: a) without image preprocessing, b) undergoes image enhancement, c) undergoes data augmentation, d) undergoes image enhancement and data

Discussion

The experimental results demonstrate that the proposed framework significantly enhances wood species identification, particularly under low-quality conditions. While standard CNNs (e.g., ResNet 50) rely heavily on distinct texture patterns, motion blur and sensor noise in industrial settings often corrupt these high-frequency details. The core mechanism of our improvement lies in the restoration of anatomical integrity via VDSR. By sharpening the boundaries of key features such as vessel pores and wood rays, the framework enables the classifier to capture discriminative spatial features that would otherwise be lost. This is evidenced by the substantial improvement in recognition accuracy for the low-quality dataset (from 56.5% to 81.5%), confirming that software-level enhancement can effectively compensate for data degradation.

In the context of existing literature, our findings highlight the importance of robustness. Recent studies such as Wu et al. (2021) and Kırbaş & Çifci (2022) have reported high accuracies (98.2% and 95.88%, respectively) on high-quality datasets using deep CNNs. Our results on the high-quality dataset (set 1) align with these benchmarks (98.2%). However, a distinct advantage of our framework is its performance retention under degradation. Standard approaches often suffer dramatic accuracy drops when processing low-quality inputs (as seen in the 56.5% baseline accuracy for set 3), whereas our method maintains a robust accuracy of 81.5%. This suggests that integrating super-resolution preprocessing is a critical strategy for real-world forestry applications where image quality cannot always be guaranteed.

From an engineering perspective, these findings have significant implications for system deployment flexibility and hardware cost optimization. The ability to achieve high accuracy with degraded inputs suggests that standard imaging devices (e.g., standard industrial cameras or handheld units) can serve as viable alternatives to expensive, high-precision imaging systems in specific scenarios. While the deep learning backend currently requires standard GPU acceleration to ensure robustness, the relaxation of stringent constraints on image acquisition hardware significantly lowers the barrier for deployment in complex environments

like log yards. Furthermore, regarding real-time feasibility, the estimated total inference latency (VDSR + ResNet 50) is approximately 50–80 ms per image on a standard GPU. This processing speed allows for sufficient sampling density on typical timber grading conveyor lines. Future work will focus on optimizing the model for edge deployment, potentially exploring lightweight architectures (e.g., MobileNet) to further reduce computational costs for handheld systems.

Conclusions

This study proposes a practical and scalable framework for wood classification in industrial environments. Incorporating VDSR and multi-scale data augmentation, the proposed method markedly enhances the recognition performance of deep learning models. This study systematically evaluated the proposed framework through the use of three visually similar wood species, thereby emulating real-world industrial application scenarios. The experimental results indicate that the proposed method exhibits robustness to fluctuations in image acquisition conditions and attains a competitive level of accuracy even when applied to low-quality images. In contrast to numerous recognition frameworks that are contingent upon high-end, precision imaging systems, the framework proposed in this study can be seamlessly integrated into industrial processes utilizing cost-effective imaging hardware (e.g., standard industrial cameras). While the current framework relies on standard GPU acceleration to ensure robustness, future research will focus on exploring lightweight architectures (e.g., MobileNet) to further reduce computational constraints, enabling deployment on resource-limited edge devices. Furthermore, future endeavors will also aim to include a more extensive array of wood species and conduct rigorous evaluations within actual production environments. Overall, the intelligent wood recognition solution proposed in this study is characterized by its reliability, cost-effectiveness, and ease of deployment, and it possesses the potential for broader application across diverse industrial domains.

Conflict of interest

The author(s) declare(s) that there is no conflict of interest concerning the publication of this article.

References

Abdul Hamid, L. B., Rosli, N. R., Mohd Khairuddin, A. S., Mokhtar, N., & Yusof, R. (2018). Denoising module for wood texture images. WOOD SCI TECHNOL, 52(6), 1539-1554. https://doi.org/10.1007/s00226-018-1049-3

Barmpoutis, P., Dimitropoulos, K., Barboutis, I., Grammalidis, N., & Lefakis, P. (2018). Wood species recognition through multidimensional texture analysis. Computers and Electronics in Agriculture, 144, 241-248. https://doi.org/10.1016/j.compag.2017.12.011

Cai, P., Zhang, Y., He, H., Lei, Z., & Gao, S. (2025). DFNet: A Differential Feature-Incorporated Residual Network for Image Recognition. J BIONIC ENG, 22(2), 931-944. https://doi.org/10.1007/s42235-025-00654-3

Chen, Y., Huang, Y., Zhang, Z., Wang, Z., Liu, B., Liu, C.,… Qian, W. (2023). Plant image recognition with deep learning: A review. COMPUT ELECTRON AGR, 212, 108072. https://doi.org/10.1016/j.compag.2023.108072

Collins-Key, S. A., Rochner, M. L., King, K. E., Kaiser, A. L., Harley, G. L., Foley, Z.,…von Arx, G. (2025). Evaluating the influence of high-resolution image capture on the signal strength of blue intensity and quantitative wood anatomy metrics from whitebark pine. Dendrochronologia, 90, 126305. https://doi.org/10.1016/j.dendro.2025.126305

Ergun, H. (2021). Segmentation of Rays in Wood Microscopy Images Using the U-Net Model. Bioresources, 16(1), 721-728. https://doi.org/10.15376/biores.16.1.721-728

Ergun, H. (2024). Wood identification based on macroscopic images using deep and transfer learning approaches. PeerJ, 12, e17021. https://doi.org/10.7717/peerj.17021

Geovanni, F. M., Erick, M. M., Carlos, V. O. J., Dagoberto, A. A., & Nelson, Z. V. (2022). Using Deep Learning to Identify Costa Rican Native Tree Species From Wood Cut Images&#13. FRONT PLANT SCI, 13, 789227-789227. https://doi.org/10.3389/fpls.2022.789227

Grimmer, G., Wenger, R., & Chardon, V. (2025). RiverDetectWood: A tool for automatic classification and quantification of river wood in river systems using aerial imagery. SoftwareX, 29, 102042. https://doi.org/10.1016/j.softx.2025.102042

Huang, L., Yao, C., Zhang, L., Luo, S., Ying, F., & Ying, W. (2024). Enhancing computer image recognition with improved image algorithms. SCI REP-UK, 14(1), 13709. https://doi.org/10.1038/s41598-024-64193-3

Kırbaş, İ., & Çifci, A. (2022). An effective and fast solution for classification of wood species: A deep transfer learning approach. Ecological Informatics, 69, 101633. https://doi.org/10.1016/j.ecoinf.2022.101633

Kobayashi, K., Hwang, S.-W., Okochi, T., Lee, W.-H., & Sugiyama, J. (2019). Non-destructive method for wood identification using conventional X-ray computed tomography data. J CULT HERIT, 38, 88-93. https://doi.org/10.1016/j.culher.2019.02.001

Koo, K.-M., & Cha, E.-Y. (2017). Image recognition performance enhancements using image normalization. HUM-CENT COMPUT INFO, 7(1), 33. https://doi.org/10.1186/s13673-017-0114-5

Li, C., Zhang, Y., Tu, W., Jun, C., Liang, H., & Yu, H. (2017). Soft measurement of wood defects based on LDA feature fusion and compressed sensor images. J FORESTRY RES, 28(6), 1285-1292. https://doi.org/10.1007/s11676-017-0395-6

Liu, L., Qiu, J., Cao, Y., Li, Q., Qian, S., & Sun, Y. (2025). An Interpretable Approach to Wood Species Identification Based on Anatomical Features in Microscopic Images. Forests, 16(8), 1328. https://doi.org/10.3390/f16081328

Lu, Z., Yao, H., Lyu, Y., He, S., Ning, H., Yu, Y.,…Zhou, L. (2024). A Deep Learning Method for Log Diameter Measurement Using Wood Images Based on Yolov3 and DeepLabv3+. Forests, 15(5).

Mallik, A., Tarrío-Saavedra, J., Francisco-Fernández, M., & Naya, S. (2011). Classification of wood micrographs by image segmentation. CHEMOMETR INTELL LAB, 107(2), 351-362. https://doi.org/10.1016/j.chemolab.2011.05.005

Nieradzik, L., Stephani, H., Sieburg-Rockel, J., Helmling, S., Olbrich, A., Wrage, S., & Keuper, J. (2024). WoodYOLO: A Novel Object Detector for Wood Species Detection in Microscopic Images. Forests, 15(11).

Pan, X., Yu, Z., & Yang, Z. (2023). A deep learning multimodal fusion framework for wood species identification using near-infrared spectroscopy GADF and RGB image. Holzforschung, 77(11-12), 816-827. https://doi.org/10.1515/hf-2023-0062 (Holzforschung)

Pan, Z., Wang, F., Luan, D., & Pan, H. (2025). Design and simulation of thermal radiation image recognition based on simulated annealing algorithm in image VR creation and acquisition system. Thermal Science and Engineering Progress, 58, 103245. https://doi.org/10.1016/j.tsep.2025.103245

Peters, R. L., Klesse, S., Bulcke, J. V. d., Jourdain, L. M. Y., Arx, G. v., Rosell, A. A.,…Mil, T. D. (2025). Quantitative vessel mapping on increment cores: a critical comparison of image acquisition methods. FRONT PLANT SCI, 16, 1502237-1502237. https://doi.org/10.3389/fpls.2025.1502237

Prabu, R., J, T. B., K, S. R., & C, W. A. (2020). The XyloTron: Flexible, Open-Source, Image-Based Macroscopic Field Identification of Wood Products. FRONT PLANT SCI, 11, 1015. https://doi.org/10.3389/fpls.2020.01015

Ravindran, P., Costa, A., Soares, R., & Wiedenhoeft, A. C. (2018). Classification of CITES-listed and other neotropical Meliaceae wood images using convolutional neural networks. Plant Methods, 14(1), 25. https://doi.org/10.1186/s13007-018-0292-9

Riana, D., Rahayu, S., Hasan, M., & Anton. (2021). Comparison of segmentation and identification of swietenia mahagoni wood defects with augmentation images. Heliyon, 7(6), e07417. https://doi.org/10.1016/j.heliyon.2021.e07417

Rosa da Silva, N., Deklerck, V., Baetens, J. M., Van den Bulcke, J., De Ridder, M., Rousseau, M.,…Verwaeren, J. (2022). Improved wood species identification based on multi-view imagery of the three anatomical planes. Plant Methods, 18(1), 79. https://doi.org/10.1186/s13007-022-00910-1

Souza, D. V., Santos, J. X., Vieira, H. C., Naide, T. L., Nisgoski, S., & Oliveira, L. E. S. (2020). An automatic recognition system of Brazilian flora species based on textural features of macroscopic images of wood. WOOD SCI TECHNOL, 54(4), 1065-1090. https://doi.org/10.1007/s00226-020-01196-z

Vijayalakshmi, S., Mrudhula, S., Ashok Kumar, V., Agastin, Varun, & Latha, A. M. (2024). Artificial Intelligence-Driven Timber Wood Defect Characterization from Terahertz Images. J NONDESTRUCT EVAL, 43(4), 116. https://doi.org/10.1007/s10921-024-01130-4

Wang, Y., Zhang, W., Gao, R., Jin, Z., & Wang, X. (2021). Recent advances in the application of deep learning methods to forestry. WOOD SCI TECHNOL, 55(5), 1171-1202. https://doi.org/10.1007/s00226-021-01309-2

Wu, F., Gazo, R., Haviarova, E., & Benes, B. (2021). Wood identification based on longitudinal section images by using deep learning. WOOD SCI TECHNOL, 55(2), 553-563. https://doi.org/10.1007/s00226-021-01261-1

Xu, W., Song, Y., Gupta, S., Jia, D., Tang, J., Lei, Z., & Gao, S. (2025). Dmixnet: a dendritic multi-layered perceptron architecture for image recognition. ARTIF INTELL REV, 58(5), 129. https://doi.org/10.1007/s10462-025-11123-y

Yang, X., Zheng, Z., Zheng, H., & Liu, X. (2024). Deep Learning Method of Precious Wood Image Classification Based on Microscopic Computed Tomography. RUSS J NONDESTRUCT+, 60(10), 1136-1148. https://doi.org/10.1134/S1061830924602447

Yang, Z., Li, Y., Bai, X., Yan, G., Sun, Q., & Fu, C. (2024). Optimal selection of key parameters for homomorphic filtering based on information entropy. MULTIMED TOOLS APPL, 83(25), 65929-65948. https://doi.org/10.1007/s11042-024-18109-y

Zhao, Z., Yang, X., Ge, Z., Guo, H., & Zhou, Y. (2021). Wood Microscopic Image Identification Method Based on Convolution Neural Network [Article]. Bioresources, 16(3), 4986-4999. https://doi.org/10.15376/biores.16.3.4986-4999

Zheng, C., Liu, S., Wang, J., Lu, Y., Ma, L., Jiao, L.,…He, T. (2024). Opening the black box: explainable deep-learning classification of wood microscopic image of endangered tree species. Plant Methods, 20(1), 56. https://doi.org/10.1186/s13007-024-01191-6

Zhang, Y., Liu, X., Liu, H., & Yu, H. (2023). MRS-Transformer: Texture Splicing Method to Remove Defects

in Solid Wood Board. Applied Sciences, 13(12), 7006. https://doi.org/10.3390/app13127006

Zhuang, Z., Liu, Y., Yang, Y., Shen, Y., & Gou, B. (2022). Color Regression and Sorting System of Solid Wood Floor. Forests, 13(9), 1454. https://doi.org/10.3390/f13091454

Zheng, Z., Ge, Z., Tian, Z., Yang, X., & Zhou, Y. (2024). WoodGLNet: a multi-scale network integrating global and local information for real-time classification of wood images. J REAL-TIME IMAGE PR, 21(4), 147. https://doi.org/10.1007/s11554-024-01521-w

Zheng, Z., Ge, Z., Zheng, H., Yang, X., Qin, L., Wang, X., & Zhou, Y. (2025). Arnet: research on wood CT image classification algorithm based on multi-scale dilated attention and residual dynamic convolution. WOOD SCI TECHNOL, 59(3), 48. https://doi.org/10.1007/s00226-025-01649-3